Journal of Environmental Chemical Engineering 14 (2026) 124005

Contents lists available at ScienceDirect

Journal of Environmental Chemical Engineering

journal homepage: www.elsevier.com/locate/jece

Optimizing CO_2 separation with PEBAX®/ionic-liquid blend membranes: A polymer grade study

Sarang Ismail [a], Julia Baron [a], Camryn Capek [a], Mostafa Dadashi Firouzjaei [a], Ahmad Arabi Shamsabadi [b], Sahar Beigzadeh [c], Habibollah Safari [a], Siamak Nejati [a], Mona Bavarian [a,*]

[a] Department of Chemical and Biomolecular Engineering, University of Nebraska-Lincoln, Lincoln, NE 68588, USA
[b] Department of Chemistry, University of Pennsylvania, Philadelphia, PA 19104, USA
[c] Department of Mechanical and Materials Engineering, University of Nebraska-Lincoln, Lincoln, NE 68588, USA

ARTICLE INFO

Keywords:
PEBAX®
Membranes
CO_2 capture
Ionic liquid
Block copolymer
Gas separation

ABSTRACT

Poly(ether-block-amide)s of various molecular weights, commercially known as PEBAX®, are shown to effectively imbibe imidazolium-based ionic liquids, forming stable quasi-solid-state phases that function as gas-separation membrane media. The results demonstrate that both the composition and molecular weight of PEBAX® provide effective handles for tuning the permeability–selectivity trade-off in CO_2/N_2 separations. Here we examine how commercial PEBAX® grades (1657, 1074, 2533, and RNEW) govern CO_2 sorption and gas transport in dense PEBAX®/ionic-liquid blend membranes containing 50 wt% 1-ethyl-3-methylimidazolium bis (trifluoromethylsulfonyl)imide, [EMIM][Tf_2N]. Fourier-transform infrared spectroscopy, X-ray diffraction, and differential scanning calorimetry indicate that IL incorporation reduces crystalline order and increases amorphous character, with the strongest performance observed for polyether-rich grades. Gravimetric sorption measurements normalized to the ionic-liquid mass show higher CO_2 uptake for PEBAX® 2533 and RNEW, reaching 3.02 ± 0.66 and 3.07 ± 0.57 mol CO_2 kg^{-1} IL, respectively, at 200 psi (1.38 MPa) and 10 °C. Pure-gas permeation at 25 °C reveals that the RNEW-based membrane combines high CO_2 permeability (618 ± 4 Barrer) with ideal CO_2/N_2 selectivity values of ≈ 55, outperforming the other grades at the same IL loading. These results establish PEBAX® grade selection as a practical design parameter for tuning dense polymer/IL blend membranes for carbon-capture separations.

1. Introduction

Anthropogenic carbon dioxide (CO_2) emissions are the dominant driver of global warming, posing one of humanity's most significant challenges in the 21st century. The excessive consumption of fossil fuels, coupled with the rapid deforestation rate, has elevated atmospheric CO_2 levels to concentrations not seen since the mid-Pliocene warm period, approximately three million years ago [1]. To mitigate the detrimental impact of global warming, a multifaceted approach is required to control CO_2 accumulation in the atmosphere, including adopting renewable energy, using low-carbon fuels, and implementing CO_2 capture and storage/utilization (CCS/CCU) technologies [2]. Among these strategies, capturing CO_2 before it enters the atmosphere offers a promising solution [3].

CO_2 separation and capture are essential to many industrial processes, including natural gas and biogas purification, syngas and hydrogen production, ammonia synthesis, flue gas treatment, and food packaging [4,5]. Accordingly, considerable research has focused on developing membranes that can enable the efficient and cost-effective separation processes. Currently, the majority of commercially available polymeric membranes for gas separation are made of glassy polymers, such as polyimide (PI), polyamide (PA), polycarbonate (PC), polysulfone (PSU), poly(phenylene oxide) (PPO), and cellulose acetate (CA) [5,6]. These materials rely on size sieving through rigid chain structures, offering desirable CO_2 selectivity values in mixtures containing larger gas molecules. However, the low CO_2 permeability values limit their applicability in large-scale industrial processes, such as syngas and flue gas treatment in power plants [5–7]. Using polymers

* Corresponding author.
E-mail address: mona.bavarian@unl.edu (M. Bavarian).

https://doi.org/10.1016/j.jece.2026.124005
Received 25 April 2026; Received in revised form 1 July 2026; Accepted 5 July 2026
Available online 8 July 2026

classified as rubber, such as poly(dimethylsiloxane) (PDMS), higher CO_2 permeabilities are obtained, which is attributed to the flexible chain structures of rubber; nevertheless, this increase in permeability comes at the expense of poor selectivity, making them unsuitable for many applications [8,9].

To address this permeability-selectivity trade-off, researchers have explored polymers containing CO_2-philic functional groups, such as ethylene oxide (EO), which interact strongly with CO_2 through dipole-quadrupole interactions. Poly(ethylene oxide) (PEO)-based materials have demonstrated excellent CO_2 selectivity values without significantly compromising permeation rates [10,11]. Strategies for incorporating polyether segments into gas separation membranes include physical blending [12–14], cross-linking [15–17], and the synthesis of PEO-based block copolymers, such as PEO-PI, PEO-PA, PEO-PBT [poly (butylene terephthalate)], PEO-PU (polyurethane), PEO-PUU [poly (urethane urea)], and PEO-PE (polyester) [18–23]. These block copolymers combine the mechanical strength, chemical resistance, and thermal stability of a semicrystalline hard phase with the CO_2-philic properties of the PEO.

Block copolymers, such as poly(ether-block-amide) PEBAX®, are particularly noteworthy for their exceptional selectivity in separating polar or quadrupolar gases (e.g., CO_2) from a mixture of non-polar gases (e.g., H_2 or N_2) [24]. The phase-separated block copolymers consist of linear chains of relatively rigid polyamide (PA) segments interspersed with flexible polyether (PE) segments. In PEBAX®, the PA block is an aliphatic polyamide, the "hard" block, e.g., nylon−6 [PA6], nylon−12 [PA12]; poly[imino(1-oxohexamethylene)], or poly[imino (1-oxododecamethylene)]) and PE is a polyether, the "soft" block, such as poly (ethylene oxide) [PEO] or poly (tetramethylene oxide) [PTMEO]. The gas transport occurs primarily through the soft polyether blocks, which exhibit high CO_2 solubility and permeability [25]. Fig. 1 provides the chemical structure of various blocks used for preparing PEBAX® allowing with the compositional information for each grade.

The PEO-based block copolymers can be used as thin films, selective coatings in composite membranes, and blends with other materials to achieve the desired mechanical and separation properties [28]. Of special interest, PEBAX® copolymers are attractive for CO_2 separations because their CO_2-philic polyether blocks, paired with mechanically robust polyamide segments, can be combined with ionic liquids to tune transport properties in dense polymer/IL media [29,30]. Dense PEBAX®/IL blend membranes can exhibit high CO_2 solubility due to the IL, while the polymer matrix provides mechanical integrity and helps retain the IL [31,32].

In the present work, [EMIM][Tf_2N] was selected as the model IL because imidazolium-based ILs are widely reported to exhibit favorable CO_2 solubility, and the Tf_2N^- anion has been shown to strongly influence CO_2 affinity in physically absorbing ILs [33,34]. In addition, imidazolium-based ILs have been used in PEBAX®-based membranes to tune microstructure and gas transport behavior, making [EMIM][Tf_2N] a suitable IL platform for dense PEBAX®/IL blend membranes [35,36]. Although other ILs may produce similar qualitative effects, the extent of crystallinity disruption and gas-transport enhancement is expected to depend on the IL cation/anion structure, viscosity, polarity, and compatibility with PEBAX® domains [36]. Therefore, [EMIM][Tf_2N] was used as a fixed IL platform to isolate the role of PEBAX® grade.

However, conventional porous-support SILMs often suffer from low CO_2 selectivity in the gaseous mixture containing low-molecular-weight light gases. Certain issues with the IL-retention stability and reproducibility have further challenged their industrial adaptability [37,38]. These limitations can be overcome by leveraging the tunable properties of PEBAX® copolymers, enabling the development of next-generation PEBAX®/IL blend membranes with enhanced performance [39,40].

In this study, we explicitly distinguish the present dense PEBAX®/IL blend membranes from conventional supported ionic liquid membranes, where the ionic liquid is immobilized within a porous support. The present membranes are homogeneous dense polymer/IL blends prepared by solution blending and solvent evaporation, not porous-support SILMs.

Prior PEBAX®/IL membrane studies have shown that IL incorporation can increase CO_2 sorption, alter crystallinity, and improve gas-transport performance (e.g., Refs [35,38]). The contribution of the present work is a controlled commercial-grade comparison at the same [EMIM][Tf_2N] loading. In this study, dense PEBAX®/IL blend membranes are introduced as tunable materials for CO_2/N_2 separation. Using PEBAX® grades 1657, 1074, 2533, and RNEW with a fixed 50 wt% [EMIM][Tf_2N] loading, we examine how commercial polymer grade affects CO_2 sorption and pure-gas transport. The manuscript focuses on the relationship among soft-segment chemistry, hard/soft block balance, crystallinity, CO_2 solubility, diffusivity, and ideal CO_2/N_2 selectivity.

The 50 wt% IL composition was used as a fixed loading to enable a controlled comparison among different PEBAX® grades. The selection of 50 wt% IL was guided by our prior systematic study on IL loading in polymeric membrane systems, where the effect of IL content on CO_2 uptake and transport behavior was evaluated and used as a benchmark for the present work [39,40].

Because PEBAX® 2533 contains PTMEO soft segments whereas RNEW is PEO-rich, this work uses "polyether" when referring to the broader soft-segment family and to distinguish PEO and PTMEO where their chemistry may affect CO_2 affinity, chain mobility, and IL compatibility.

2. Experimental methods

2.1. Material

PEBAX® polymer pellets (Arkema USA) of different grades, including 1657, 1074, 2533, and RNEW, were generously supplied by Arkema (USA). The imidazolium-based ionic liquid, 1-ethyl−3-methylimidazolium bis(trifluoromethylsulfonyl) imide ([EMIM][Tf_2N]), with a minimum purity of 98%, was sourced from Sigma-Aldrich (St. Louis, MO, USA). Alcohol solvents employed in this study, specifically ethanol, 1-propanol, and 1-butanol, each with a minimum purity of 99%, were also obtained from Sigma-Aldrich (St. Louis, MO, USA). A high-purity carbon dioxide gas cylinder (CO_2, Coleman Instrument grade, purity > 99.99%) was procured from Matheson Tri-Gas, Inc. (Lincoln, NE, USA). Additionally, 6 MHz Gold AT quartz crystals (QCs) featuring a polished

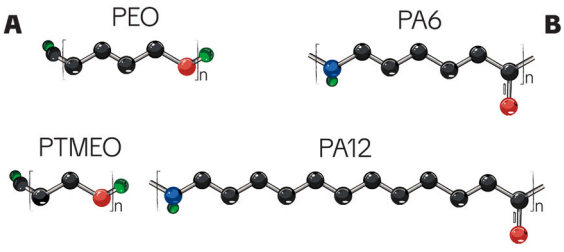

B

PEBAX® Grade	Hard Block (Polyamide)/wt.%	Soft Block (Polyether)/wt.%
1657	PA6/40%	PEO/60%
1074	PA12/45%	PEO/55%
2533	PA12/20%	PTMEO/80%
RNEW® 30R51	PA11/19%	PEO/81%

Fig. 1. A) Ball and stick representation of the chemical structures of PEBAX® blocks and B) the weight percentage distribution of hard (Polyamide) and soft (Polyether) blocks in different PEBAX® grades [26,27]. .

surface were acquired from PhillipTech (Greenville, SC, USA). The Eon-LT Monitor, part of the quartz crystal microbalance (QCM) sensor system, specifically the Phoenix Temperature Monitoring Sensor System with an Eon-LT Monitor, was provided by Colnatec Inc., based in Gilbert, AZ, USA.

2.2. Solution preparation and PEBAX®/IL blend preparation

To investigate CO_2 sorption in PEBAX®/IL blend membranes, polymer/IL mixtures were prepared by solution blending. Initially, a 4 wt% PEBAX® 1657 solution was prepared in ethanol/water (3:1 v/v), heated to 80 °C, and stirred at 400 rpm for 24 h. After cooling to ambient temperature, predetermined amounts of [EMIM][Tf_2N] were added to prepare PEBAX® 1657 blends containing 10, 30, and 50 wt% IL. The mixtures were reheated to 80 °C and stirred at 400 rpm for 24 h before film preparation.

Initially, IL compatibility with the block copolymer was evaluated by preparing PEBAX®/IL blend solutions containing 30, 50, and 70 wt% IL and measuring CO_2 sorption. Beyond 50 wt% IL, the sorption behavior showed no significant further improvement, similar to what we observed in our previous report [41]. Therefore, the PEBAX®/IL blend membrane containing 50 wt% IL was selected to investigate the CO_2 sorption capacity of various PEBAX® grades.

For CO_2 sorption analysis, polymeric solutions of PEBAX® grades 1657, 1074, 2533, and RNEW with 4, 2, 2, and 2 wt% were prepared in (3:1) v/v mixtures of ethanol/water, 1-propanol/ ethanol, and 1-propanol/1-butanol, respectively. The mixtures were heated and stirred at 80 °C and 400 rpm for 24 h. Then, the solutions were cooled to room temperature, and the required amount of IL was added to obtain a final composition of 50 wt% IL.

2.3. Thin-film fabrication and free-standing film casting

Thin films of polymers, ranging from 100 to 200 nanometers in thickness, were prepared by spin coating of the PEBAX®/IL blend solutions on QC substrates at room temperature. The specific spin-coating conditions are in the supporting information (SI), Section 1. The substrates were heated under vacuum at 60 °C for 30 min, followed by annealing at 80 °C for ≈ 38 h. Similar to thin-film fabrication, the free-standing films were prepared by heating and stirring all solutions at 80 °C and 400 rpm for 24 h. Subsequently, the solutions were poured into PTFE Petri dishes (80 mm diameter, 28 mm depth). The cast films were first placed in a preheated vacuum oven at 60 °C, and the temperature was gradually increased to 80 °C at a ramp rate of 1.3 °C/min. The films were kept at 80 °C for 24 h to remove residual solvent. After that, a vacuum was applied using a rotary vane pump, and the drying continued for another 24 h. The samples were stored in the vacuum oven until use. Free-standing films were prepared for Fourier-transform infrared spectroscopy (FTIR), X-ray diffraction (XRD), differential scanning calorimetry (DSC), and gas permeation testing.

For gas permeation measurements, free-standing cast membranes were used instead of the 100–200 nm thin films prepared for QCM analysis. The free-standing membranes had an average thickness of 339 ± 150 μm. Permeability was calculated using a membrane test area of 33.18 cm^2, with the upstream side pressurized to 0.1 MPa and the downstream side maintained under vacuum at approximately 0.05 Pa.

2.4. Characterizations

2.4.1. FTIR

Membrane samples were characterized using a TENSOR II Fourier-transform infrared (FTIR) spectrometer (Bruker, Karlsruhe, Germany) in attenuated total reflection (ATR) mode over the range of 400–1700 cm^{-1}.

2.4.2. XRD

The X-ray Diffractometer by Rigaku SmartLab (Rigaku Co., Tokyo, Japan) with Cu K_α radiation at 40 kV and 40 mA voltage and current settings examined the crystalline structures of the entire membranes. Intensities were measured from 10° to 45° angular range, at a scanning rate of 1°/min with step scans at intervals of 0.05°.

2.4.3. DSC

Thermal transitions of the neat PEBAX® grades and PEBAX®/[EMIM][Tf_2N] blend membranes were characterized using a DSC 204 F1 Phoenix instrument. Samples weighing 8–10 mg were placed in aluminum crucibles and heated from −80 to 250 °C at a rate of 5 °C min^{-1} under a nitrogen purge of 10 mL min^{-1} . The glass-transition temperature (T_g) was determined from the midpoint of the heat-capacity change, while melting temperatures (T_m) were determined from the maxima of the corresponding endothermic transitions. DSC was used to compare the positions, widths, and relative intensities of the thermal transitions in the neat and IL-containing polymers; DSC-derived crystallinity values were not calculated. Quantitative crystallinity indices were determined separately from XRD peak-deconvolution analysis.

2.4.4. CO_2 Solubility

The CO_2 solubility using the gravimetric sorption method in PEBAX®/IL blend membranes was performed on a modified setup of QCM. The point adsorption isotherms and enthalpy of adsorption measurements were conducted using the experimental setup and procedures reported in our previous work [42]. .

2.4.5. SEM

Post-permeation membrane surface morphology was examined using a FEI Helios NanoLab 660 field-emission scanning electron microscope under the imaging conditions described in the Supporting Information.

2.4.6. Gas permeability measurement

CO_2 and N_2 permeation rates were measured at 25 °C by the differential pressure method to determine the transport behavior of pure gases. The measurements were taken with the Gas Permeability Tester G101, manufactured by Saicheng Electronic Technology Co., Ltd., China. This equipment operates in accordance with several international standards, including ISO 15105–1 and ISO 2556, which detail methods for determining the gas transmission rate of films and sheeting, as well as JIS K7126–1 and ASTM D1434–23, which provide guidelines for films and plastics. Free-standing cast membranes were used for permeation testing with an average thickness of 339 ± 150 μm, with an effective test area of 33.18 cm^2. While testing, the upstream chamber was pressurized with pure gas at 0.1 MPa, while the downstream chamber was maintained under vacuum at approximately 0.05 Pa.

The downstream pressure increase was monitored over time, and the steady-state linear region of the pressure-time curve was used to calculate the gas transmission rate and permeability. The time lag, θ, was obtained by extrapolating the linear portion of the curve to the time axis, and the diffusion coefficient was calculated using $D = l^2/6\theta$. The solubility coefficient was determined from the solution–diffusion relationship, $S = P/D$, and ideal selectivity was calculated from the ratio of pure-gas permeability values. For each PEBAX® grade, 20 permeation data points were collected to evaluate measurement reproducibility. The uncertainties associated with permeability, diffusivity, solubility, and ideal selectivity were estimated using standard error propagation.

3. Results and discussion

3.1. Effect of ionic liquid confinement and PEBAX® composition on CO_2 solubility

Fig. 2 A shows the FTIR spectra of the IL-embedded PEBAX® grades (1657, 1074, 2533, and RNEW), which differ in hard/soft-block composition. The spectra display the characteristic H–N–C═O band at 1638 cm^{-1}, assigned to the PA block, and the C–O–C band at 1100 cm^{-1}, corresponding to the polyether block [27,43]. Among the studied grades, PEBAX® 2533 and RNEW (with higher polyether content) show more pronounced changes in the C–O–C region, while comparatively smaller changes are observed in the PA-related peak. FTIR confirms IL incorporation, while the combined DSC, XRD, and sorption results suggest greater structural perturbation of polyether-rich domains.

Fig. 2B further shows the CO_2 sorption uptake (mol CO_2 kg^{-1} IL) for different PEBAX®/IL blend membranes over a pressure range of 50–200 psi at 10 °C. PEBAX® 2533 and RNEW exhibit the highest CO_2 uptake, reaching 3.02 ± 0.66 and 3.07 ± 0.57 mol CO_2 kg^{-1} IL, respectively, at 200 psi, whereas PEBAX® 1657 and 1074 show lower 10 °C uptake values of 2.62 ± 0.16 and 2.53 ± 0.08 mol CO_2 kg^{-1} IL, respectively. The higher CO_2 solubility in 2533 and RNEW is therefore consistent with their polyether-rich composition. These results suggest that IL incorporation enhances CO_2 sorption primarily through compatibility between the IL and polyether-rich domains. Prior studies attribute IL-polyether compatibility to the interactions involving ether oxygens and imidazolium/[Tf_2N] species [44,45]. These interactions disrupt polyether-chain ordering and reduce crystallinity, promoting a more amorphous morphology with greater chain flexibility and free volume, favoring gas transport [8,46]. In addition, the ether groups in PEO- and PTMEO-containing domains have strong affinity toward CO_2 due to dipole-quadrupole interactions, a phenomenon well-documented in ether-based polymers [29,46]. As the polyether phase becomes more amorphous, the accessibility of these ether groups increases, further improving CO_2 solubility. Overall, the combined FTIR, DSC, XRD, and sorption results support the interpretation that IL-embedded PEBAX® membranes with higher polyether content, particularly PTMEO-containing PEBAX® 2533 and PEO-rich PEBAX® RNEW, provide superior CO_2 solubility performance. This makes them promising candidates for CO_2 separation applications, where high sorption capacity and favorable transport properties are desired [47]. .

The sorption isotherms in Fig. 2**B** were measured at 10 °C, whereas pure-gas permeation was measured at 25 °C. Therefore, the sorption data are used primarily to compare grade-dependent uptake trends rather than to calculate a direct solubility-permeability relationship at the permeation temperature. Table S2 provides sorption data measured at 10, 20, 30, and 40 °C, together with values linearly interpolated to 25 °C. The results show that CO_2 uptake decreases as temperature increases, while the relative performance ranking of the PEBAX® grades remains unchanged.

3.2. Thermal Properties and Crystallinity of PEBAX®/IL blend membranes

Fig. 3A shows the DSC thermograms of the PEBAX®/IL blend membranes. All samples exhibit a glass transition temperature (T_g) at approximately −50 °C, assigned to the polyether soft block [48]. In addition, PEBAX® 2533 shows a melting transition near −14 °C, which is attributed to the PTMEO component in the soft segment [49], while PEBAX® RNEW displays an endothermic transition near 9 °C, corresponding to the melting of PEO domains [50]. These low-temperature transitions indicate semicrystalline behavior in the soft segments.

To directly evaluate the effect of IL incorporation, DSC thermograms of the corresponding neat PEBAX®, shown in Figure S3, are compared with the blend. The neat polymers show well-resolved grade-dependent thermal transitions associated with both the soft polyether domains and the hard polyamide domains. Neat PEBAX® 1657 exhibits melting transitions near 16 °C and 203 °C, assigned to the PEO and PA domains, respectively. Neat PEBAX® 1074 shows corresponding transitions near 14 °C and 160 °C, while neat PEBAX® 2533 exhibits a PTMEO-related melting transition near −15 °C and a PA-domain transition near 174 °C. For neat PEBAX® RNEW, the PEO melting transition appears near 17 °C, with a PA-related transition near 151 °C.

Compared with the neat polymers, the PEBAX®/IL blend membranes exhibit broader, weaker, and in some cases shifted thermal transitions. For example, the PEO melting transition of RNEW shifts from approximately 17 °C in the neat polymer to approximately 9 °C after IL incorporation, while the PA-domain transition of 1657 shifts from approximately 203 °C to approximately 186 °C. In 2533, the PTMEO transition remains near −14 to −15 °C but appears less distinct, whereas the PA-domain transitions in several IL-containing membranes become broadened or partially suppressed. These changes indicate that [EMIM][Tf_2N] alters the thermal organization of both the polyether and polyamide domains and reduces the definition of their melting transitions.

The altered DSC profiles are consistent with IL-induced disruption of intermolecular interactions within PEBAX®, including ion–dipole interactions with the polyether segments and interference with hydrogen bonding among the polyamide domains. Similar behavior has been reported for PEBAX®/IL systems containing [BMIM][Tf_2N], [BMIM][CF_3SO_3], and [EMIM][Tf_2N], where IL incorporation reduces

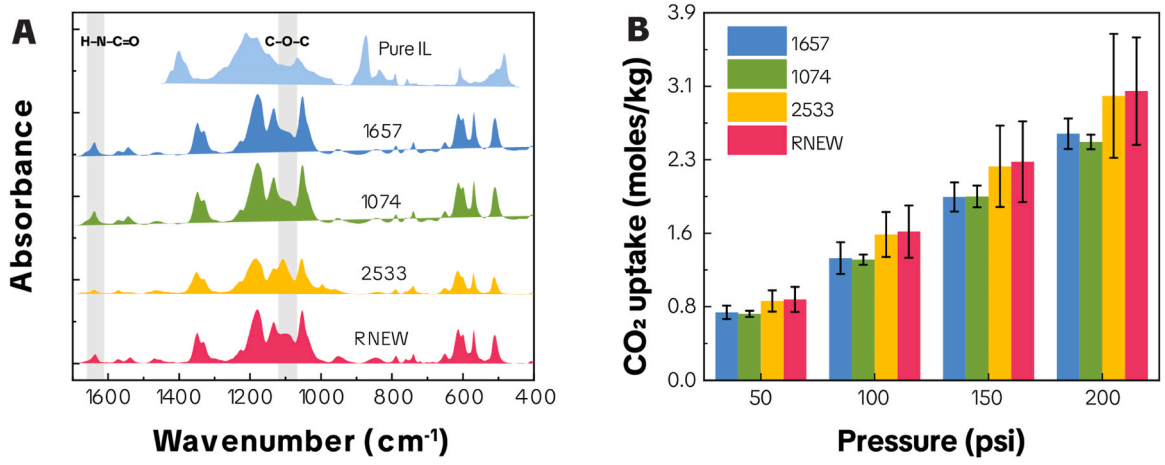

Fig. 2. (A) FTIR spectra of neat [EMIM][Tf_2N], and PEBAX®/IL blend membranes. (B) CO_2 adsorption isotherms for PEBAX®/IL blend membranes containing 50 wt % [EMIM][Tf_2N], with uptake normalized as mol CO_2 kg^{-1} IL.

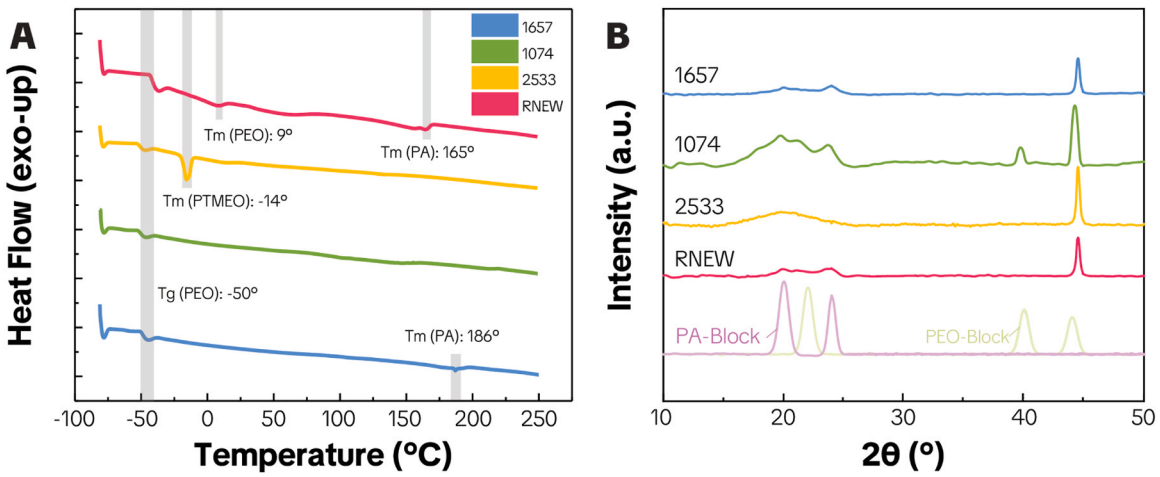

Fig. 3. (A) DSC thermograms of [EMIM][Tf₂N]-embedded PEBAX®/IL blend membranes (1657, 1074, 2533, RNEW). (B) XRD patterns of PEBAX®/IL blend membranes, highlighting the influence of IL incorporation on polymer crystallinity.

crystallinity by disrupting chain packing and crystallization kinetics [47, 51–54]. Overall, the reduction, broadening, and shifting of thermal transitions support partial amorphization and reduced crystal order in the PEBAX®/[EMIM][Tf₂N] blend membranes. This increased amorphous character is expected to enhance membrane flexibility and facilitate gas sorption and transport.

Fig. 3B shows the XRD patterns of the PEBAX®/IL blend membranes. In PEBAX®-based systems, reflections in the 2θ ≈ 20–24° region are generally associated with crystalline PA domains, while features near 2θ ≈ 22–23° and 40–45° are attributed to crystalline polyether phases, including PEO/PTMEO domains [55–57]. After IL incorporation, all PEBAX®/IL blend membranes exhibit reduced peak intensity and broader diffraction features, indicating lower crystallinity. This effect is especially evident for the polyether-related peaks (≈22° and ≈44°), which are diminished or shifted, suggesting disruption of the regular polyether crystalline lattice. In contrast, the PA-related peaks at ≈ 20° and 24° remain visible but with reduced intensity, indicating partial retention of PA crystallinity.

To provide a direct grade-specific comparison, XRD patterns of neat PEBAX® 1657, 1074, 2533, and RNEW are provided in Figure S4, and the crystallinity index values are summarized in Table S5. Peak deconvolution shows that crystallinity decreases from 54 to 84% for the neat PEBAX® grades to 36–41% after IL incorporation. For example, the crystallinity of PEBAX® 1657 decreases from 54% in the neat polymer to 36% in the corresponding PEBAX®/IL membrane. These results confirm that the IL disrupts crystalline packing across all PEBAX® grades,

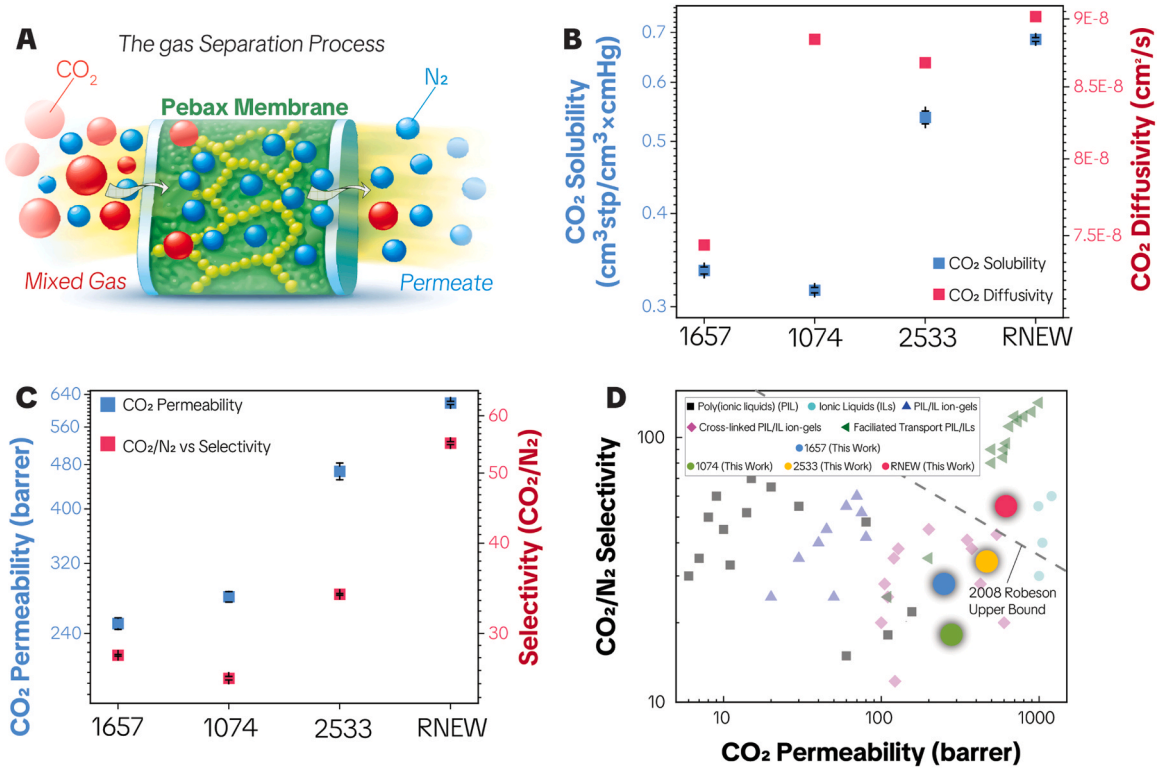

Fig. 4. Influence of PEBAX® grade on CO_2 permeability, ideal selectivity, and gas-transport properties in dense PEBAX®/IL blend membranes. (A) Schematic representation of the PEBAX®/IL blend membrane concept. (B) CO_2 solubility and diffusivity in PEBAX®/IL blend membranes. (C) CO_2 permeability and ideal CO_2/N_2 selectivity. (D) Literature comparison of CO_2 transport performance with IL-containing PEBAX®, polymer/IL gel, and related IL-based membranes.

leading to partial amorphization, particularly within the polyether-rich domains, while some PA-domain ordering is retained.

This trend is consistent with stronger compatibility between [EMIM][Tf_2N] and the polyether segments through ion–dipole interactions with ether oxygen atoms, which disturbs chain packing and limits crystallization. The PA domains retain partial crystallinity, likely due to their stronger interchain interactions and lower compatibility with the IL [57]. Overall, the XRD results support the DSC findings and confirm IL-induced reduction of crystalline order in the PEBAX®/IL membranes, which is expected to influence membrane flexibility and gas transport behavior.

3.3. Gas permeation

Fig. 4 summarizes the pure-gas permeation performance of the free-standing dense PEBAX®/IL blend membranes at 1 bar and 25 °C, including CO_2 permeability, diffusivity, solubility, and CO_2/N_2 ideal selectivity. In Fig. 4**C**, the PEBAX® RNEW-based PEBAX®/IL blend membrane shows the highest CO_2 permeability (618 ± 4 Barrer) and maintains 55 CO_2/N_2 selectivity. PEBAX® 2533, despite having a polyether-rich composition distinct from RNEW, exhibits lower CO_2 permeability but retains competitive selectivity (~34). PEBAX® 1657 and 1074 show intermediate performance, with CO_2 permeability values of 250 ± 6 and 279 ± 6 Barrer and CO_2/N_2 selectivity values of 28 and 26, respectively. Because the membranes tested here were free-standing dense films with an average thickness of 339 ± 150 μm, permeability is reported as the primary transport metric; however, the corresponding CO_2 permeance values calculated from the measured thickness are provided in Table S7, ranging from 0.737 to 1.823 GPU. As a representative neat-polymer control, neat PEBAX® 2533 was tested under the same permeation protocol (Table S8). Incorporation of 50 wt% [EMIM][Tf_2N] increased CO_2 permeability from 265 ± 2–467 ± 16 Barrer and CO_2/N_2 ideal selectivity from 19 to 34 ± 0.15, supporting improved CO_2 transport in the PTMEO-rich 2533 matrix. Because this comparison was performed only for PEBAX® 2533, it is presented as a representative control rather than a grade-wide neat-polymer comparison.

Fig. 4B separates the solubility and diffusivity contributions to overall CO_2 permeability. It was found that RNEW grade is not simply diffusion-driven: both CO_2 diffusivity and CO_2 solubility increase relative to PEBAX® 1657. For example, PEBAX® 1657 shows a diffusivity of 7.4×10^{-8} cm^2 s^{-1} and a solubility of 0.34 ± 0.0081 cm^3 (STP) cm^{-3} $cmHg^{-1}$, whereas PEBAX® RNEW shows a diffusivity of 9.0×10^{-8} cm^2 s^{-1} and a solubility of 0.68 ± 0.0044 cm^3 (STP) cm^{-3} $cmHg^{-1}$. The solubility increase is especially important and is consistent with greater accessible CO_2-philic ether/IL-rich domains, while the diffusivity increase is consistent with reduced crystalline constraints and increased segmental mobility. Thus, the high RNEW permeability arises from coupled solubility and diffusivity enhancement rather than from diffusivity alone. Fig. 4**D** compares these membranes with IL-containing PEBAX® and related polymer/IL membrane systems [39,55–57]. .

These results indicate that CO_2 separation performance in PEBAX®/IL blend membranes is strongly dependent on polymer composition, soft-segment chemistry, and microstructure. The superior RNEW performance is consistent with a PEO-rich soft phase that provides accessible CO_2-philic sorption sites and sufficient segmental mobility, while the PA-rich domains retain mechanical integrity. In contrast, PEBAX® 2533 contains PTMEO soft segments, which is not chemically identical to PEO even though both are polyethers.

Permeation stability under the tested conditions was assessed by collecting at least 20 continuous permeation data points for each PEBAX® grade, including RNEW, under identical testing conditions. The stable pressure-rise response indicated consistent membrane performance without evidence of defect formation or failure. Post-permeation FTIR spectra in Figure S2 in SI, confirmed the retention of characteristic IL bands, supporting IL retention and suggesting that IL leaching did not significantly affect the measured gas transport properties. In addition, post-permeation SEM images of two independently prepared PEBAX® RNEW/IL membranes showed continuous surfaces without visible tears, cracks, delamination, or pinholes in Figure S6 in SI, further supporting preservation of membrane integrity during testing.

4. Conclusion

This study shows that the commercial PEBAX® grade can serve as an effective design parameter for tuning dense PEBAX®/ionic-liquid blend membranes containing 50 wt% [EMIM][Tf_2N]. Among the grades investigated, PEBAX® RNEW exhibited the best pure-gas CO_2/N_2 separation performance, with a CO_2 permeability of 618 ± 4 Barrer and an ideal CO_2/N_2 selectivity of approximately 55. This enhanced performance is associated with increased CO_2 solubility and diffusivity, which arise from the combined effects of accessible CO_2-philic polyether domains, IL-rich sorption environments, and reduced crystalline constraints.

Supporting information

The supporting information is available free of charge.

CRediT authorship contribution statement

Mona Bavarian: Writing – review & editing, Validation, Supervision, Software, Resources, Project administration, Methodology, Conceptualization. **Sarang Ismail:** Writing – original draft, Visualization, Investigation, Formal analysis, Data curation. **Julia Baron:** Investigation, Formal analysis. **Habibollah Safari:** Data curation, Writing – review & editing. **Camryn Capek:** Investigation, Formal analysis. **Sahar Beigzadeh:** Data curation, Formal analysis, Writing – review & editing. **Mostafa Dadashi Firouzjaei:** Writing – review & editing, Visualization, Conceptualization. **Ahmad Arabi Shamsabadi:** Writing – review & editing, Methodology, Conceptualization. **Siamak Nejati:** Writing – review & editing, Validation, Supervision, Resources, Conceptualization.

Declaration of Competing Interest

The authors declare that they have no known competing financial interests or personal relationships that could have appeared to influence the work reported in this paper.

Acknowledgement

The authors acknowledge the support of the American Chemical Society-Petroleum Research Fund (ACS-PRF) under the award number #66227-DNI4. The research was performed in part in the Nebraska Nanoscale Facility: National Nanotechnology Coordinated Infrastructure and the Nebraska Center for Materials and Nanoscience, which are supported by the National Science Foundation under Award ECCS: 1542182, and the Nebraska Research Initiative.

Appendix A. Supporting information

Supplementary data associated with this article can be found in the online version at doi:10.1016/j.jece.2026.124005.

Data availability

Data will be made available on request.

References

[1] M. Willeit, A. Ganopolski, R. Calov, A. Robinson, M. Maslin, The role of CO2 decline for the onset of Northern Hemisphere glaciation, Quat. Sci. Rev. 119 (Jul. 2015) 22–34, https://doi.org/10.1016/j.quascirev.2015.04.015.

[2] F. Nocito, A. Dibenedetto, Atmospheric CO2 mitigation technologies: carbon capture utilization and storage, Curr. Opin. Green. Sustain. Chem. 21 (Feb. 2020) 34–43, https://doi.org/10.1016/j.cogsc.2019.10.002.

[3] V. Eke, T. Sahu, K.K. Ghuman, M. Freire-Gormaly, P.G. O'Brien, A comprehensive review of life cycle assessments of direct air capture and carbon dioxide storage, Sustain. Prod. Consum. 55 (May 2025) 217–241, https://doi.org/10.1016/j.spc.2025.02.017.

[4] H. Yang, et al., Progress in carbon dioxide separation and capture: A review, J. Environ. Sci. 20 (1) (Jan. 2008) 14–27, https://doi.org/10.1016/S1001-0742(08)60002-9.

[5] A.D. Ebner, J.A. Ritter, State-of-the-art Adsorption and Membrane Separation Processes for Carbon Dioxide Production from Carbon Dioxide Emitting Industries, Sep. Sci. Technol. 44 (6) (Apr. 2009) 1273–1421, https://doi.org/10.1080/01496390902733314.

[6] R.W. Baker, Future Directions of Membrane Gas Separation Technology, Ind. Eng. Chem. Res. 41 (6) (Mar. 2002) 1393–1411, https://doi.org/10.1021/ie0108088.

[7] D.F. Sanders, et al., Energy-efficient polymeric gas separation membranes for a sustainable future: A review, Polymer 54 (18) (Aug. 2013) 4729–4761, https://doi.org/10.1016/j.polymer.2013.05.075.

[8] Y. Wang, H. Li, G. Dong, C. Scholes, V. Chen, Effect of Fabrication and Operation Conditions on CO2 Separation Performance of PEO–PA Block Copolymer Membranes, Ind. Eng. Chem. Res. 54 (29) (Jul. 2015) 7273–7283, https://doi.org/10.1021/acs.iecr.5b01234.

[9] T.C. Merkel, V.I. Bondar, K. Nagai, B.D. Freeman, I. Pinnau, Gas sorption, diffusion, and permeation in poly(dimethylsiloxane), J. Polym. Sci. Part B Polym. Phys. 38 (3) (2000) 415–434, https://doi.org/10.1002/(SICI)1099-0488(20000201)38:3<415::AID-POLB8>3.0.CO;2-Z.

[10] M.K. Barillas, R.M. Enick, M. O'Brien, R. Perry, D.R. Luebke, B.D. Morreale, The CO2 permeability and mixed gas CO2/H2 selectivity of membranes composed of CO2-philic polymers, J. Membr. Sci. 372 (1) (Apr. 2011) 29–39, https://doi.org/10.1016/j.memsci.2011.01.028.

[11] H. Lin, B.D. Freeman, Materials selection guidelines for membranes that remove CO2 from gas mixtures, J. Mol. Struct. 739 (1) (Apr. 2005) 57–74, https://doi.org/10.1016/j.molstruc.2004.07.045.

[12] J. Li, K. Nagai, T. Nakagawa, S. Wang, Preparation of polyethyleneglycol (PEG) and cellulose acetate (CA) blend membranes and their gas permeabilities, J. Appl. Polym. Sci. 58 (9) (1995) 1455–1463, https://doi.org/10.1002/app.1995.070580906.

[13] J. Li, S. Wang, K. Nagai, T. Nakagawa, A.W.-H. Mau, Effect of polyethyleneglycol (PEG) on gas permeabilities and permselectivities in its cellulose acetate (CA) blend membranes, J. Membr. Sci. 138 (2) (Jan. 1998) 143–152, https://doi.org/10.1016/S0376-7388(97)00212-3.

[14] M. Sadeghi, M. Pourafshari Chenar, M. Rahimian, S. Moradi, A.H.S. Dehaghani, Gas permeation properties of polyvinylchloride/polyethyleneglycol blend membranes, J. Appl. Polym. Sci. 110 (2) (2008) 1093–1098, https://doi.org/10.1002/app.28740.

[15] Y. Hirayama, Y. Kase, N. Tanihara, Y. Sumiyama, Y. Kusuki, K. Haraya, Permeation properties to CO2 and N2 of poly(ethylene oxide)-containing and crosslinked polymer films, J. Membr. Sci. 160 (1) (Jul. 1999) 87–99, https://doi.org/10.1016/S0376-7388(99)00080-0.

[16] H.-Y. Zhao, Y.-M. Cao, X.-L. Ding, M.-Q. Zhou, J.-H. Liu, Q. Yuan, Poly(ethylene oxide) induced cross-linking modification of Matrimid membranes for selective separation of CO2, J. Membr. Sci. 320 (1) (Jul. 2008) 179–184, https://doi.org/10.1016/j.memsci.2008.03.070.

[17] H. Lin, et al., Transport and structural characteristics of crosslinked poly(ethylene oxide) rubbers, J. Membr. Sci. 276 (1) (May 2006) 145–161, https://doi.org/10.1016/j.memsci.2005.09.040.

[18] H.B. Park, C.K. Kim, Y.M. Lee, Gas separation properties of polysiloxane/polyether mixed soft segment urethane urea membranes, J. Membr. Sci. 204 (1) (Jul. 2002) 257–269, https://doi.org/10.1016/S0376-7388(02)00048-0.

[19] D. Husken, T. Visser, M. Wessling, R.J. Gaymans, CO2 permeation properties of poly(ethylene oxide)-based segmented block copolymers, J. Membr. Sci. 346 (1) (Jan. 2010) 194–201, https://doi.org/10.1016/j.memsci.2009.09.034.

[20] H. Li, B.D. Freeman, O.M. Ekiner, Gas permeation properties of poly(urethane-urea)s containing different polyethers, J. Membr. Sci. 369 (1) (Mar. 2011) 49–58, https://doi.org/10.1016/j.memsci.2010.11.024.

[21] W. Yave, A. Szymczyk, N. Yave, Z. Roslaniec, Design, synthesis, characterization and optimization of PTT-*b*-PEO copolymers: A new membrane material for CO2 separation, J. Membr. Sci. 362 (1) (Oct. 2010) 407–416, https://doi.org/10.1016/j.memsci.2010.06.060.

[22] M. Yoshino, K. Ito, H. Kita, K.-I. Okamoto, Effects of hard-segment polymers on CO2/N2 gas-separation properties of poly(ethylene oxide)-segmented copolymers, Journal Polymer Science Part B Polymer Physics 38 (13) (2000) 1707–1715, https://doi.org/10.1002/1099-0488(20000701)38:13<1707::AID-POLB40>3.0.CO;2-W.

[23] S.R. Reijerkerk, A. Arun, R.J. Gaymans, K. Nijmeijer, M. Wessling, Tuning of mass transport properties of multi-block copolymers for CO2 capture applications, J. Membr. Sci. 359 (1) (Sep. 2010) 54–63, https://doi.org/10.1016/j.memsci.2009.09.045.

[24] V.I. Bondar, B.D. Freeman, I. Pinnau, Gas transport properties of poly(ether-b-amide) segmented block copolymers, Journal Polymer Science Part B Polymer Physics 38 (15) (2000) 2051–2062, https://doi.org/10.1002/1099-0488(20000801)38:15<2051::AID-POLB100>3.0.CO;2-D.

[25] B.D. Freeman, I. Pinnau, Polymeric Materials for Gas Separations, vol. 733, in ACS Symposium Series, in: Polymer Membranes for Gas and Vapor Separation, 733, American Chemical Society, 1999, pp. 1–27, https://doi.org/10.1021/bk-1999-0733.ch001. vol. 733, in ACS Symposium Series.

[26] R. Surya Murali, A. Jha, Aarti, S. Divekar, S. Dasgupta, Synthesis and characterization of a high-performance bio-based Pebax membrane for gas separation applications, Mater. Adv. 4 (20) (2023) 4843–4851, https://doi.org/10.1039/D3MA00385J.

[27] L. Martínez-Izquierdo, A. Perea-Cachero, M. Malankowska, C. Téllez, J. Coronas, A comparative study between single gas and mixed gas permeation of polyether-block-amide type copolymer membranes, J. Environ. Chem. Eng. 10 (5) (Oct. 2022) 108324, https://doi.org/10.1016/j.jece.2022.108324.

[28] Y. Wang, T. Hu, H. Li, G. Dong, W. Wong, V. Chen, Enhancing Membrane Permeability for CO2 Capture Through Blending Commodity Polymers with Selected PEO and PEO-PDMS Copolymers and Composite Hollow Fibres, Energy Procedia 63 (Jan. 2014) 202–209, https://doi.org/10.1016/j.egypro.2014.11.021.

[29] A.S. Embaye, L. Martínez-Izquierdo, M. Malankowska, C. Téllez, J. Coronas, Poly (ether-block-amide) Copolymer Membranes in CO2 Separation Applications, Energy Fuels 35 (21) (Nov. 2021) 17085–17102, https://doi.org/10.1021/acs.energyfuels.1c01638.

[30] J.A. Piotrowska, C. Jordan, M. Harasek, K. Bica-Schröder, Development of Hollow Fiber Membranes Functionalized with Ionic Liquids for Enhanced CO2 Separation, ACS Sustain. Chem. Eng. 12 (32) (Aug. 2024) 12236–12248, https://doi.org/10.1021/acssuschemeng.4c04597.

[31] J. Wang, J. Luo, S. Feng, H. Li, Y. Wan, X. Zhang, Recent development of ionic liquid membranes, Green. Energy & Environ. 1 (1) (Apr. 2016) 43–61, https://doi.org/10.1016/j.gee.2016.05.002.

[32] M. Ramdin, T.W. de Loos, T.J.H. Vlugt, State-of-the-Art of CO2 Capture with Ionic Liquids, Ind. Eng. Chem. Res. 51 (24) (Jun. 2012) 8149–8177, https://doi.org/10.1021/ie3003705.

[33] C. Cadena, J.L. Anthony, J.K. Shah, T.I. Morrow, J.F. Brennecke, E.J. Maginn, Why Is CO2 So Soluble in Imidazolium-Based Ionic Liquids? J. Am. Chem. Soc. 126 (16) (Apr. 2004) 5300–5308, https://doi.org/10.1021/ja039615x.

[34] J.L. Anthony, J.L. Anderson, E.J. Maginn, J.F. Brennecke, Anion effects on gas solubility in ionic liquids, J. Phys. Chem. B 109 (13) (Apr. 2005) 6366–6374, https://doi.org/10.1021/jp046404l.

[35] P. Bernardo, et al., Gas transport properties of Pebax®/room temperature ionic liquid gel membranes, Sep. Purif. Technol. 97 (Sep. 2012) 73–82, https://doi.org/10.1016/j.seppur.2012.02.041.

[36] Z. Dai, R.D. Noble, D.L. Gin, X. Zhang, L. Deng, Combination of ionic liquids with membrane technology: A new approach for CO2 separation, J. Membr. Sci. 497 (Jan. 2016) 1–20, https://doi.org/10.1016/j.memsci.2015.08.060.

[37] L.C. Tomé, I.M. Marrucho, Ionic liquid-based materials: a platform to design engineered CO2 separation membranes, Chem. Soc. Rev. 45 (10) (May 2016) 2785–2824, https://doi.org/10.1039/C5CS00510H.

[38] S. Pishva, S. Hassanajili, Investigation on effect of ionic liquid on CO2 separation performance and properties of novel co-casted dual-layer PEBAX-ionic liquid/PES composite membrane, J. Ind. Eng. Chem. 107 (Mar. 2022) 180–196, https://doi.org/10.1016/j.jiec.2021.11.046.

[39] S. Ismail, et al., Polymer Molecular Weight as a Tuning Parameter for Enhancing CO2 Separation Performance in Supported Ionic Liquid Membranes, ACS Appl. Polym. Mater. 7 (18) (Sep. 2025) 12441–12449, https://doi.org/10.1021/acsapm.5c02276.

[40] S. Ismail, H. Safari, M. Bavarian, Design of Supported Ionic Liquid Membranes for CO2 Capture Using a Generative AI-Based Approach, Ind. Eng. Chem. Res. (Feb. 2025), https://doi.org/10.1021/acs.iecr.4c03280.

[41] L. Martínez-Izquierdo, C. Téllez, J. Coronas, Highly stable Pebax® Renew® thin-film nanocomposite membranes with metal organic framework ZIF-94 and ionic liquid [Bmim][BF4] for CO2 capture, J. Mater. Chem. A 10 (36) (Sep. 2022) 18822–18833, https://doi.org/10.1039/D2TA03958C.

[42] T.-H. Wang, L.-W. Hsu, H.-C. Chang, Structural Reorganization of Imidazolium Ionic Liquids Induced by Pressure-Enhanced Ionic Liquid—Polyethylene Oxide Interactions, Int. J. Mol. Sci. 22 (2) (Jan. 2021) 981, https://doi.org/10.3390/ijms22020981.

[43] K. Kodama, et al., Structural effects of polyethers and ionic liquids in their binary mixtures on lower critical solution temperature liquid-liquid phase separation, Polym. J. 43 (3) (Mar. 2011) 242–248, https://doi.org/10.1038/pj.2010.140.

[44] S. Bandehali, A. Moghadassi, F. Parvizian, S.M. Hosseini, T. Matsuura, E. Joudaki, Advances in high carbon dioxide separation performance of poly (ethylene oxide)-based membranes, J. Energy Chem. 46 (Jul. 2020) 30–52, https://doi.org/10.1016/j.jechem.2019.10.019.

[45] T. Narkkun, W. Kraithong, S. Ruangdit, C. Klaysom, K. Faungnawakij, V. Itthibenchapong, Pebax/Modified Cellulose Nanofiber Composite Membranes for Highly Enhanced CO2/CH4 Separation, ACS Omega 8 (48) (Dec. 2023) 45428–45437, https://doi.org/10.1021/acsomega.3c04800.

[46] S.J. Metz, M.H.V. Mulder, M. Wessling, Gas-Permeation Properties of Poly (ethylene oxide) Poly(butylene terephthalate) Block Copolymers, Macromolecules 37 (12) (Jun. 2004) 4590–4597, https://doi.org/10.1021/ma049847w.

[47] J.H. Kim, S.Y. Ha, Y.M. Lee, Gas permeation of poly(amide-6-*b*-ethylene oxide) copolymer, J. Membr. Sci. 190 (2) (Sep. 2001) 179–193, https://doi.org/10.1016/S0376-7388(01)00444-6.

[48] G. Clarizia, et al., Heterogenized Imidazolium-Based Ionic Liquids in Pebax®Rnew. Thermal, Gas Transport and Antimicrobial Properties, Art. no. 6, Polymers 12 (6) (Jun. 2020), https://doi.org/10.3390/polym12061419.

[49] Y. Qiu, J. Ren, D. Zhao, H. Li, M. Deng, Poly(amide-6-*b*-ethylene oxide)/[Bmim][Tf2N] blend membranes for carbon dioxide separation, J. Energy Chem. 25 (1) (Jan. 2016) 122–130, https://doi.org/10.1016/j.jechem.2015.10.009.

[50] Anja Car, Chrtomir Stropnik, W. Yave, K.-V. Peinemann, PEG modified poly(amide-*b*-ethylene oxide) membranes for CO2 separation, J. Membr. Sci. 307 (1) (Jan. 2008) 88–95, https://doi.org/10.1016/j.memsci.2007.09.023.

[51] Y. Kumar, S.A. Hashmi, G.P. Pandey, Lithium ion transport and ion–polymer interaction in PEO based polymer electrolyte plasticized with ionic liquid, Solid. State Ion. 201 (1) (Oct. 2011) 73–80, https://doi.org/10.1016/j.ssi.2011.08.010.

[52] S. Wang, et al., Pebax–PEG–MWCNT hybrid membranes with enhanced CO2 capture properties, J. Membr. Sci. 460 (Jun. 2014) 62–70, https://doi.org/10.1016/j.memsci.2014.02.036.

[53] "Gas sorption and characterization of poly(ether-b-amide) segmented block copolymers - Bondar - 1999 - Journal of Polymer Science Part B: Polymer Physics - Wiley Online Library." Accessed: Jul. 09, 2024. [Online]. Available: https://onlinelibrary.wiley.com/doi/abs/10.1002/(SICI)1099-0488(19990901)37:17%3C2463::AID-POLB18%3E3.0.CO;2-H.

[54] J. Muroga, E. Kamio, A. Matsuoka, K. Nakagawa, T. Yoshioka, H. Matsuyama, Development of an ion gel-based CO 2 separation membrane composed of Pebax 1657 and a CO 2 -philic ionic liquid, RSC Adv. 14 (29) (2024) 20786–20796, https://doi.org/10.1039/D3RA08730A.

[55] D. Chen, W. Ying, Y. Guo, Y. Ying, X. Peng, Enhanced Gas Separation through Nanoconfined Ionic Liquid in Laminated MoS2 Membrane, ACS Appl. Mater. Interfaces 9 (50) (Dec. 2017) 44251–44257, https://doi.org/10.1021/acsami.7b15762.

[56] Y. Han, W.S.W. Ho, Polymeric membranes for CO2 separation and capture, J. Membr. Sci. 628 (Jun. 2021) 119244, https://doi.org/10.1016/j.memsci.2021.119244.

[57] W. Ying, et al., Ionic Liquid Selectively Facilitates CO2 Transport through Graphene Oxide Membrane, ACS Nano 12 (6) (Jun. 2018) 5385–5393, https://doi.org/10.1021/acsnano.8b00367.